

Short Communication

On the Temperature Dependence of Hydrogen Evolution Reaction at Pt-modified Nickel Foam Catalyst Material

*Boguslaw Pierozynski**, *Tomasz Mikolajczyk*

Department of Chemistry, Faculty of Environmental Management and Agriculture, University of Warmia and Mazury in Olsztyn, Plac Lodzki 4, 10-957 Olsztyn, Poland

*E-mail: bogpierzynski@yahoo.ca, boguslaw.pierzynski@uwm.edu.pl

Received: 14 September 2015 / *Accepted:* 2 October 2015 / *Published:* 4 November 2015

This article presents the temperature-dependence of hydrogen evolution reaction (HER), studied at Pt-modified nickel foam material in 0.1 M NaOH solution for the temperature range: 20-60 °C. Catalytically-modified (by spontaneous Pt deposition) nickel foam exhibited radical facilitation of the HER kinetics (examined by means of a.c. impedance spectroscopy), as compared to those recently reported on pure and Pd-activated Ni foam samples. The presence of a catalytic, nanoparticle Pt additive was demonstrated through a combined SEM/EDX examination.

Keywords: Nickel foam; Catalytic Pt modification; HER; Electrochemical impedance spectroscopy

1. INTRODUCTION

Hydrogen evolution reaction (HER) on metal-based cathodes constitutes one of the most important electrochemical processes, essential when rapid development of PEM (Proton Exchange Membrane) fuel-cell technology is concerned. Simultaneously, nickel is one of the most promising catalysts amongst non-noble materials suitable for cathodic evolution of hydrogen in alkaline media, mostly because of its superior corrosion resistance at high pH values [1-5]. Nickel foams [6, 7] are characterized by high porosity and large specific surface area. In addition, these materials possess high electrical conductivity and exceptional mechanical durability [7, 8]. Considerable improvement of electrocatalytic HER properties of nickel foam could be achieved via surface modification by nanostructured noble metals, including: Pt, Ru, Rh, Pd and their alloys. This could be realized by means of electrodeposition, spontaneous deposition [8-13] or by chemical reduction processes [14-19]. In this communication, temperature-dependent HER characteristics of Pt-modified nickel foam (via

spontaneous deposition) are presented, comparatively to those of as received and Pd-activated Ni foam catalyst materials, as recently reported in other publications from this laboratory [20, 21].

2. EXPERIMENTAL

Pure nickel foam sheet was acquired from MTI Corporation (purity: > 99.99 % Ni; thickness: 1.6 mm; surface density: 346 g m^{-2} ; porosity: $\geq 95 \%$). Spontaneous deposition of Pt (see details on the spontaneous Pd/Ru deposition on Ni foam substrate given in Ref. 16) on nickel foam samples (*ca.* $1.1 \times 1.1 \text{ cm}$) was performed from chloroplatinic acid hexahydrate (CPAH, Sigma-Aldrich) solution (0.0005 M CPAH, pH= 1.0, $t_{\text{dep.}} = 30 \text{ s}$, $T_{\text{dep.}} = 293 \text{ K}$, $m_s = 41.2 \text{ mg}$ with estimated 0.18 wt.% Pt).

Electrochemical a.c. impedance experiments were performed by means of *Solartron 12,608 W* Full Electrochemical System (1260 frequency response analyzer and 1287 electrochemical interface) over the temperature range: 20-60 °C. A suitable correction was introduced [22], in order to account for a small, but considerable temperature shift of the Pd RHE over the studied temperature range. All other information concerning: preparation of electrolytes, electrochemical cell, counter and reference electrodes, as well as specific pre-treatments applied to these electrodes and employed protocols for electrochemical measurements have recently been discussed in other works from our laboratory [20, 21]. In addition, SEM/EDX spectroscopic characterization of examined Pt-based Ni foam samples was performed by means of JEOL JSM-7600F/X-Max SDD Oxford Inca 250 integrated SEM/EDX equipment unit.

3. RESULTS AND DISCUSSION

3.1. SEM/EDX characterization of Pt-activated nickel foam electrode

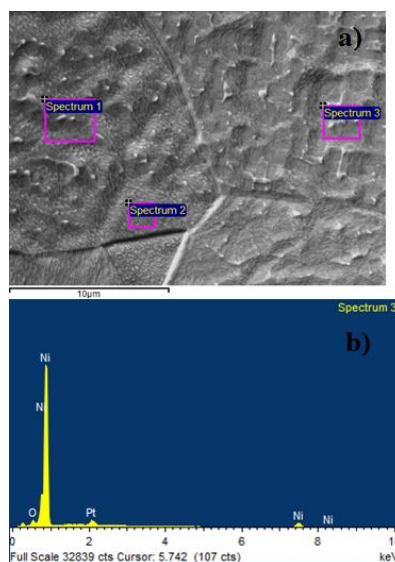


Figure 1. a) SEM micrograph picture of Pt-modified Ni foam surface (*ca.* 0.18 wt.% Pt), taken at $3,500\times$ magnification; b) EDX spectrum for Pt-modified Ni foam substrate.

Fig. 1a above presents SEM picture of Pt-modified (*ca.* 0.18 wt.% Pt) nickel foam electrode, recorded for a magnification of 3,500 \times and an acceleration voltage of 2 kV. The presence of small Pt nuclei could clearly be observed in this figure. On the other hand, Fig. 1b refers to Pt detection on the Ni foam substrate, achieved by the SEM/EDX analysis. The amount of Pt catalyst deposited on the nickel foam substrate was evaluated by means of a weighing method, where levels of nickel dissolved during the Pt deposition process were spectroscopically estimated (via a complexometric method by means of WTW Photo Flex Turb spectrometer). Furthermore, SEM-estimated (see again Refs. 20 and 21 for details) Pt average grain size came to 9.1 ± 3.1 nm.

3.2. A.c. impedance behaviour of HER on Pt-activated Ni foam material in 0.1 M NaOH

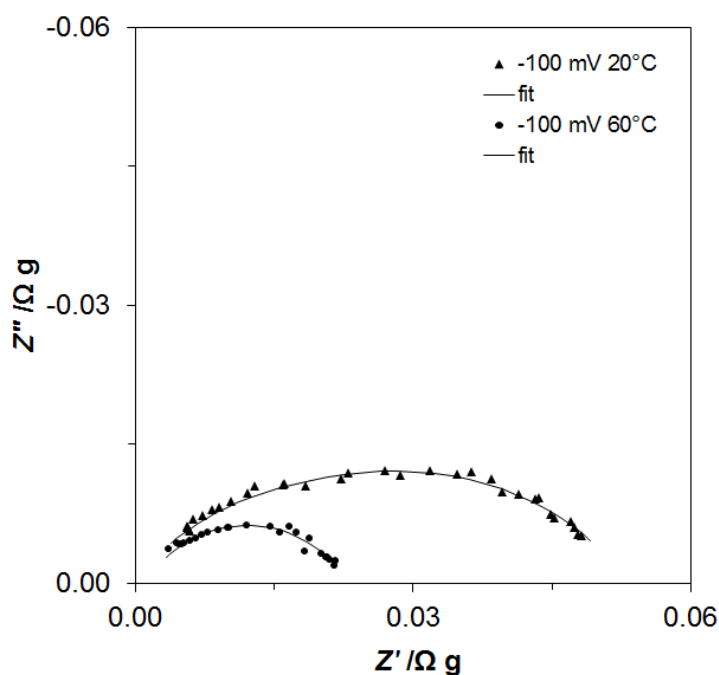


Figure 2. Complex-plane impedance plots for the HER on Pt-activated Ni foam electrode surface in contact with 0.1 M NaOH, recorded at 20 and 60 °C for -100 mV vs. RHE. Symbols represent experimental results; solid lines correspond to representation of the data according to CPE-modified Randles equivalent circuit.

A.c. impedance characterization of the HER on Pt-modified Ni foam electrode in 0.1 M NaOH is shown in Fig. 2 and Table 1. The impedance-studied Pt-activated Ni foam electrode exhibited a single-step charge-transfer reaction (single, “depressed” semicircles) at all examined potentials and reaction temperatures, in the explored frequency range. Examples of Nyquist impedance plots, recorded on the Pt-modified Ni foam electrode at -100 mV vs. RHE for two extremes of reaction temperature (20 and 60 °C) are presented in Fig. 2. It should also be noticed that a high-frequency semicircle (electrode porosity response typically observed in alkaline media) was practically undetectable in the Nyquist plots.

Table 1. Electrochemical parameters for the HER on Pt-activated Ni foam electrode in contact with 0.1 M NaOH, recorded at 20 and 60 °C. The results were obtained by fitting the CPE-modified Randles equivalent circuit to the experimentally obtained impedance data (reproducibility usually below 10 %, $\chi^2 = 3 \times 10^{-4}$ to 2×10^{-3} ; dimensionless φ parameter, which determines the constant phase angle in the complex-plane plot of the CPE circuit, oscillated between 0.45 and 0.83).

<i>E</i> /mV	<i>R</i> _{ct} /Ω g	
	20 °C	60 °C
-50	0.067 ± 0.002	0.021 ± 0.001
-100	0.056 ± 0.001	0.021 ± 0.007
-150	0.053 ± 0.001	0.020 ± 0.001
-200	0.048 ± 0.001	0.019 ± 0.004
-250	0.046 ± 0.001	0.018 ± 0.000
-300	0.040 ± 0.001	0.019 ± 0.006
-350	0.040 ± 0.004	0.017 ± 0.003
	<i>C</i> _{dl} /μF g ⁻¹ s ^{φ-1}	
-50	1,214,805 ± 112,509	1,340,655 ± 219,331
-100	682,063 ± 39,793	284,174 ± 33,893
-150	547,791 ± 61,798	285,352 ± 15,212
-200	262,597 ± 38,864	184,463 ± 33,500
-250	268,713 ± 32,245	158,339 ± 12,958
-300	158,082 ± 17,680	148,708 ± 13,819
-350	126,259 ± 30,302	129,910 ± 11,092

Faradaic reaction resistance (*R*_{ct}) and double-layer capacitance (*C*_{dl}) parameters for the HER, recorded on the platinum-modified nickel foam (at 20 and 60 °C) in function of cathodic overpotential, are presented in Table 1. Electrochemical parameters were derived based on a constant phase element – CPE-modified Randles equivalent circuit model (see e.g. Fig. 4a in Ref. 20), where the CPE element was used in the circuit in order to account for the capacitance dispersion effect [23, 24], represented by deformed semicircles in the Nyquist impedance plots of Fig. 2.

Hence, for the Pt-activated Ni foam electrodes the recorded *R*_{ct} parameter decreased from 0.067 and 0.021 Ω g at -50 mV to reach 0.040 and 0.017 Ω g at -350 mV for 20 and 60 °C, correspondingly. Simultaneously, the *C*_{dl} parameter significantly reduced from 1,214,805 to 126,259 μF g⁻¹s^{φ-1} at 20 °C and from 1,340,655 to 129,910 μF g⁻¹s^{φ-1} at 60 °C for the same overpotential range. The latter, radical *C*_{dl} reduction effect results from partial blocking of electrochemically active electrode surface by

newly formed H₂ bubbles, especially evident at increasing cathodic overpotentials. These results are in contrast to those recently recorded on the Pd-modified Ni foam in Ref. 21. Hence, at the overpotential of -50 mV, the Pt-activated foam electrode exhibited nearly 22.8× diminished the R_{ct} parameter (and *ca.* 5.9× increased C_{dl}) at room temperature, as compared to that of the Pd-modified nickel foam catalyst. Hence, having subtracted the effect of electrochemically accessible surface extension, it could be assumed that for two similar catalytic systems, the Pt-based electrode is *ca.* 4 times as catalytic for the HER (at an initial overpotential value) as the palladium-activated Ni foam material. Similar trend is observed at another potential extreme (-350 mV), where the surface-normalized (based on the recorded ratio of the double-layer capacitance parameter) enhancement of the HER kinetics for the Pt-activated Ni foam (in relation to that of the Pd-modified foam material) came to 5.2× at 20 °C and 10.5× at 60 °C (see Table 1 here and Table 2 of Ref. 21 for details). However, superior HER kinetics on the platinum-modified nickel foam electrode (being in a stationary mode) results in a rapid reduction of the electrochemically available surface area, due to extensive accumulation of hydrogen microbubbles (contrast to the behaviour observed at less catalytic Pd-activated Ni foam [21]). As a consequence, the HER kinetics recorded in Table 1 for 60 °C was practically overpotential independent. Further enhancement of the HER kinetics for this spongy-type cathode arrangement would require that e.g. an ultrasonic or a mechanical H₂ bubble removal setup be imposed.

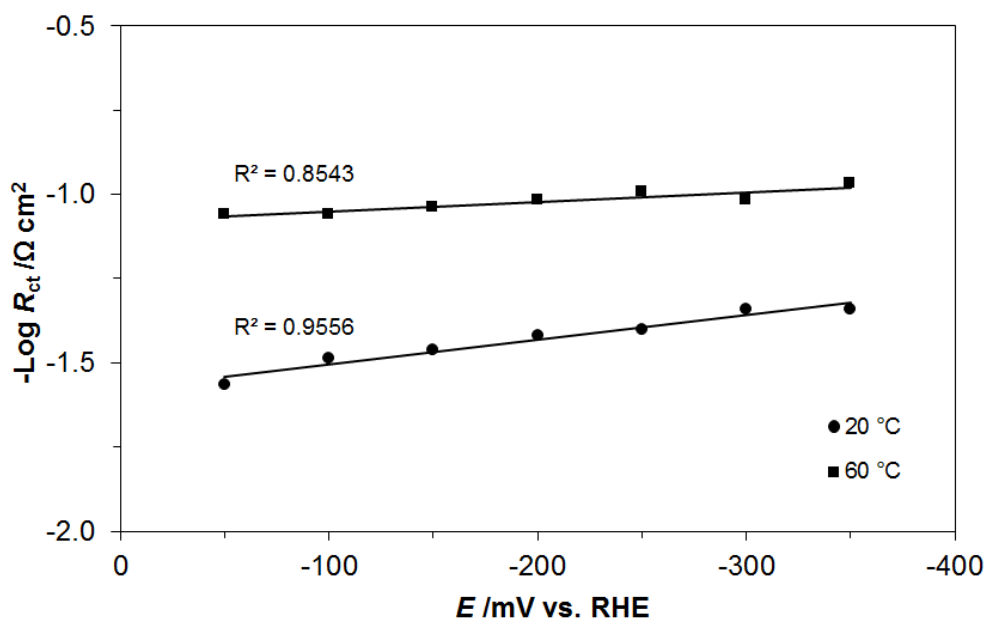


Figure 3. Linear plots of $-\log R_{ct}$ in function of potential (vs. RHE), obtained for the HER on Pt-modified Ni foam electrode in 0.1 M NaOH solution, recorded at 20 and 60 °C (symbols refer to experimental results; solid lines are data fits).

Furthermore, exchange current-densities (j_0) for the HER were calculated based on the Butler-Volmer equation and by utilizing the relation between the exchange current-density and the R_{ct} parameter for overpotential approaching zero value [5, 25-27]. The linear relationship: $-\log R_{ct}$ versus overpotential was exhibited over the examined potential range: -50 through -350 mV vs. RHE (Fig. 3).

Thus, the impedance-originated values of the j_0 parameter for the Pt-modified nickel foam electrode came to: 3.3×10^{-4} and 1.2×10^{-3} A cm $^{-2}$ at 20 and 60 °C, respectively. These results are in contrast with radically lower values of the exchange current-density, recently recorded [21] on pure and the Pd-activated nickel foam electrodes, namely: 1.2×10^{-6} and 2.0×10^{-5} A cm $^{-2}$ (Ni foam cathode), and 1.3×10^{-5} and 1.4×10^{-4} A cm $^{-2}$ for the palladium-modified cathode for 20 and 60 °C, correspondingly. Most importantly, the impedance-estimated values of the j_0 parameter for highly-dispersed, nanoparticle Pt/Ni foam composite electrode came fairly close to that widely accepted j_0 (3×10^{-4} to 7×10^{-4} A cm $^{-2}$) in literature for polycrystalline Pt, Pt(hkl) and Pt/C hydrogen evolution catalysts in alkaline media [28-30]. It should also be stated here that the recorded in this work values of the j_0 parameter for the Pt-modified nickel foam were significantly greater than those commonly quoted for Ni porous structures in literature, including: pure and Ru-modified Ni foam [20], (La, Ce)/Ni electrodes [31], electrodeposited porous Ni layers [10], etc.

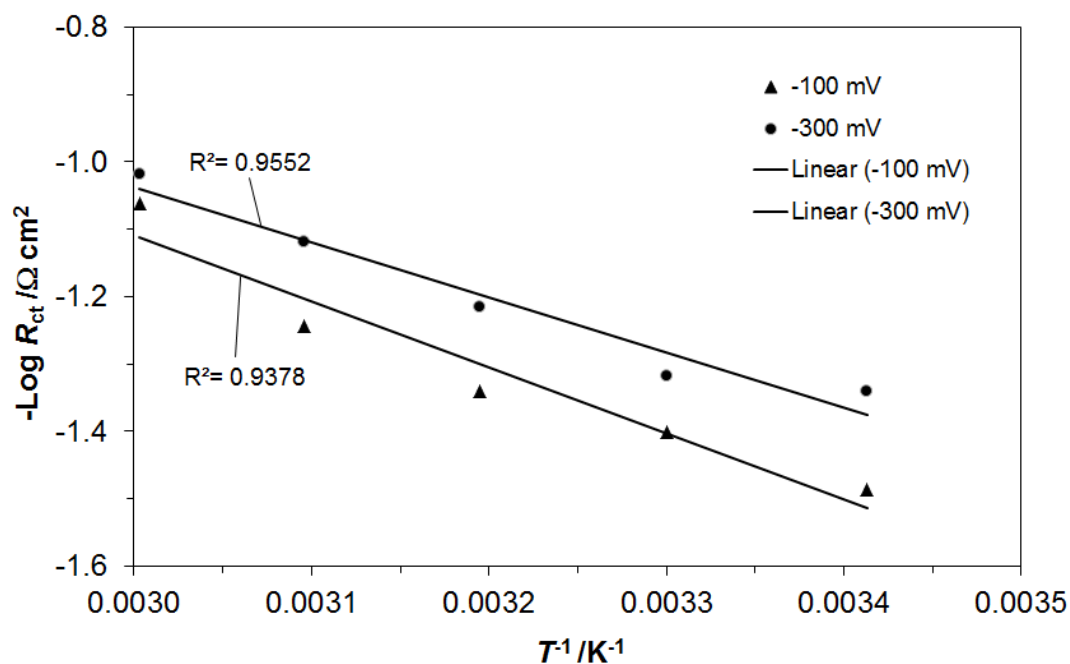


Figure 4. Plots of $-\log R_{ct}$ vs. T^{-1} for the HER conducted on Pt-modified Ni foam electrode in 0.1 M NaOH solution, at the overpotential values of -100 and -300 mV.

In addition, Fig. 4 illustrates $-\log R_{ct}$ vs. T^{-1} Arrhenius-type plots, constructed based on the $R_{ct}=f(T)$ impedance results, presented for two overpotentials (-100 and -300 mV) on the Pt-activated Ni foam catalyst electrode. Hence, experimentally-derived, electrochemical energies of activation, E_A [kJ mol $^{-1}$] for the HER came to 18.7 and 15.7 kJ mol $^{-1}$ for -100 and -300 mV, correspondingly (compare with 45.4 and 14.6 kJ mol $^{-1}$ derived for pure Ni foam cathode, and 34.3 and 13.6 kJ mol $^{-1}$ recorded for the Pd-activated Ni foam electrode [21], at the respective overpotential values).

4. CONCLUSIONS

Platinum-activated Ni foam material (Pt nanodeposit at *ca.* 0.18 wt.%) demonstrated radically enhanced catalytic HER activity in alkaline solution (based on the recorded exchange current-density and electrochemical activation energy parameters), as compared to those of as received and Pd-modified nickel foam cathodes. The above was observed over kinetically-controlled, low overpotential range, being primarily a result of exceptional HER activity of a catalytic Pt additive. However, superior HER kinetics on the Pt-modified catalyst led to substantial blockage of its electrochemically active surface, being especially challenging at most cathodic overpotentials. Hence, proper surface restoration treatment would be required (e.g. realized by means of an intermittent ultrasonic procedure or through rapid and continuous electrolyte flow) in order to maintain electrode's HER catalytic properties at high and relatively constant level.

Finally, the results obtained in this article indicated major prospects for Pt nanodeposit-modified (at nearly trace catalyst level) nickel foam cathodes in commercial alkaline water electrolyser technology.

References

1. B.E. Conway and B.V. Tilak, *Adv. Catal.*, 38 (1992) 1.
2. J.Y. Huot and L. Brossard, *Int. J. Hydrogen Energy*, 12(12) (1987) 821.
3. H.E.G. Rommal and P.J. Morgan, *J. Electrochem. Soc.*, 135(2) (1988) 343.
4. D.M. Soares, O. Teschke and I. Torriani, *J. Electrochem. Soc.*, 139(1) (1992) 98.
5. N. Krstajic, M. Popovic, B. Grgur, M. Vojnovic and D. Sepa, *J. Electroanal. Chem.*, 512 (2001) 16.
6. V. Paserin, S. Marcuson, J. Shu and D.S. Wilkinson, *Adv. Eng. Mater.*, 6 (2004) 454.
7. S. Inazawa, A. Hosoe, M. Majima and K. Nitta, *SEI Tech. Rev.*, 71 (2010) 23.
8. E. Verlato, S. Cattarin, N. Comisso, A. Gambirasi, M. Musiani and L. Vazquez-Gomez, *Electrocatalysis*, 3 (2012) 48.
9. I. Bianchi, E. Guerrini and S. Trasatti, *Chem. Phys.*, 319 (2005) 192.
10. L. Vazquez-Gomez, S. Cattarin, P. Guerriero and M. Musiani, *Electrochim. Acta*, 53 (2008) 8310.
11. S. Fiameni, I. Herraiz-Cardona, M. Musiani, V. Perez-Herranz, L. Vazquez-Gomez and E. Verlato, *Int. J. Hydrogen Energy*, 37 (2012) 10507.
12. Y. Liu, C.M. Hangarter, D. Garcia and T.P. Moffat, *Surf. Sci.*, 631 (2015) 141.
13. X. Qian, T. Hang, S. Shanmugam and M. Li, *ACS Appl. Mater. Interfaces*, 7 (2015) 15716.
14. P. Kim, J.B. Joo, W. Kim, J. Kim, I.K. Song and J. Yi, *J. Power Sources*, 160 (2006) 987.
15. Y. Suo and I.M. Hsing, *J. Power Sources*, 196 (2011) 7945.
16. A. Dutta, S.S. Mahapatra and J. Datta, *Int. J. Hydrogen Energy*, 36 (2011) 14898.
17. R.M. Modibedi, T. Masombuka and M.K. Mathe, *Int. J. Hydrogen Energy*, 36 (2011) 4664.
18. B. Beyribey, B. Corbacioglu and Z. Altin, *GUJS*, 22(4) (2009) 351.
19. J. van Drunen, B.K. Pilapil, Y. Makonnen, D. Beauchemin, B.D. Gates and G. Jerkiewicz, *ACS Appl. Mater. Interfaces*, 6 (2014) 12046.
20. B. Pierozynski, T. Mikolajczyk and I.M. Kowalski, *J. Power Sources*, 271 (2014) 231.
21. B. Pierozynski and T. Mikolajczyk, *Electrocatalysis*, 6 (2015) 51.
22. A. Prokopowicz and M. Opallo, *Solid State Ionics*, 157 (2003) 209.
23. T. Pajkossy, *J. Electroanal. Chem.*, 364(1-2) (1994) 111.
24. B.E. Conway and B. Pierozynski, *J. Electroanal. Chem.*, 622 (2008) 10.

25. J.G. Highfield, E. Claude and K. Oguro, *Electrochim. Acta*, 44 (1999) 2805.
26. R.K. Shervedani and A.R. Madram, *Electrochim. Acta*, 53 (2007) 426.
27. S. Martinez, M. Metikos-Hukovic and L. Valek, *J. Mol. Cat. A: Chem.*, 245 (2006) 114.
28. T.J. Schmidt, P.N. Ross Jr. and N.M. Markovic, *J. Electroanal. Chem.*, 524-525 (2002) 252.
29. W. Sheng, H.A. Gasteiger and S.H. Yang, *J. Electrochem. Soc.*, 157(11) (2010) B1529.
30. B.E. Conway and B.V. Tilak, *Electrochim. Acta*, 47 (2002) 3571.
31. M.A. Dominguez-Crespo, A.M. Torres-Huerta, B. Brachetti-Sibaja and A. Flores-Vela, *Int. J. Hydrogen Energy*, 36 (2011) 135.

© 2015 The Authors. Published by ESG (www.electrochemsci.org). This article is an open access article distributed under the terms and conditions of the Creative Commons Attribution license (<http://creativecommons.org/licenses/by/4.0/>).